Journal of Sound and Vibration (2001) **242**(2), 277–293
doi:10.1006/jsvi.2000.3354, available online at http://www.idealibrary.com on IDEAL®

COMPUTER SIMULATION OF THE DYNAMIC AND VIBRATION RESPONSE OF A BELT DRIVE PULLEY

P. M. SINGRU

Department of Mechanical Engineering, Rajeev Gandhi College of Engineering Research and Technology, Chandrapur, MS 442402, India. E-mail: pravinsingru@hotmail.com

AND

J. P. MODAK

Department of Mechanical Engineering and Dean Research and Development, Priyadarshini College of Engineering, Nagpur, MS, India

(*Received* 13 *December* 1999, *and in final form* 22 *August* 2000)

Torque transmitted from rim to the shaft through the arms of the pulley is analyzed in this paper. Dynamic and vibration response of the arm of the pulley of a belt drive is studied by transferring the system to equivalent spring, mass and damper system. The number of arms present in the load zone is assumed to take charge of the load zone angle equally as they appear in the load zone. Hence, the arms are subjected to stepped load wave. The arm is considered as a tapered cantilever beam fixed at the hub and stepped loading at the rim end. Response of this equivalent system is studied by varying equivalent damping coefficient from 0 to 5·0. This investigation aims at getting a cursory idea of the maximum stress due to vibration.

The natural frequency of equivalent system is compared with that of tapered cantilever beam to check its accuracy.

1. INTRODUCTION

Belts are used to transmit power between two parallel shafts. A certain minimum distance must separate the shafts, which is dependent upon the type of belt used, in order to work most efficiently. Flat-belt drives are quiet and absorb more torsional vibrations from the system than either gears or V-belt [1].

Firbank [2] explains the theory of flat belt drives in the following way:

> *A change in belt tension due to friction forces between the belt and pulley will pass the belt to elongate or contract and move relative to the surface of the pulley.*

This motion is caused by elastic creep and is associated with sliding friction as opposed to static friction. For the driving pulley, the belt first contacts the pulley with a tight-side tension (T_t) and the velocity V_t, which is the same as the surface velocity of pulley. At the end of the effective arc, the belt leaves that pulley with a loose-side tension T_s and a reduced velocity V_s.

The relation between T_t and T_s is given by

$$T_t = T_s e^{\mu\phi}. \tag{1}$$

0022-460X/01/170277 + 17 $35.00/0

Power transmitted is given by

$$P = (T_t - T_s)V. \tag{2}$$

A flat-belt drive is designed by limiting the maximum tension T_t according to the permissible tensile stress specified for the belt material [1]. Pulley material is generally cast iron or cast steel. Pulleys with less than 100-mm diameter are like solid discs. Pulleys with diameter less than 600 mm, have four arms and for diameter more than 600 mm, have six arms. The cross-section of the arm is elliptical with the major axis equal to twice the minor axis. The cross-section of the arm is obtained by considering the arm as a cantilever, fixed at the hub and carrying a concentrated load at the rim end. The length of the cantilever is taken to be equal to the radius of the pulley.

In the case of the driven pulley, it is assumed that, at any given time, the power is transmitted from the hub to the rim, through half the total number of arms. The reason put forth, for this assumption, is that the rim is not sufficiently thick and so it cannot distribute the load amongst all the arms.

This practice is followed in the design of pulleys of flat-belt drives [3–5]. Failure of the arm is not reported from the industry. Hence, the design is done till date on this assumption. Saraph *et al.* [6] presented a three-dimensional finite element stress analysis of a sheave and its experimental verification. But this analysis is also a verification of the same assumption. Only static loading is considered in this work.

So far, vibration response of an arm of the pulley of a belt drive has not yet been reported in the literature. This paper is the first attempt. Hence, this investigation aims at getting a cursory idea of the maximum stress due to vibration.

2. PROBLEM FORMULATION

The portion of the rim, in the active load zone, is subjected to non-linearly varying frictional force as per equation (1). Hence, the arms are subjected to varying load. But in design procedure, it is assumed that the torque transmitted is equally shared by about half the number of arms. The reason given for this assumption is that the rim is not sufficiently thick, so it cannot distribute the load among all the arms. By equation (1), it seems that this assumption is unrealistic. Also, there is no generalized mathematical formulation correlating load variation of an arm as a function of its position, rim thickness, pulley diameter, number of arms, loading condition and rim material properties. Hence, it is impossible to predict the limit of thin rim assumption.

Modak *et al.* [7], stated that:

(1) Increase in rim thickness may reduce the range of variation of the armload.
(2) The arms outside the load zone must be contributing to the torque transmission.

The mechanism of torque transmission from the rim to the shaft through the arms of a driven pulley is also suggested in this work [7]. Three approaches are suggested to analyze this mechanism.

(1) Equal distribution of load zone by the arms based on highly simplifying assumption.
(2) Equilibrium of the rim portion in the load zone.
(3) Finite element analysis of the pulley.

This paper deals with the analysis of the mechanism of torque transmission from the rim to the shaft through the arms of the pulley by the first approach, viz., equal distribution of the load zone by the arms.

2.1. EQUAL DISTRIBUTION OF THE LOAD ZONE BY THE ARMS

This is the first of the three above-stated approaches for analyzing the mechanism of torque transmission of a driven pulley of a belt drive. This approach is based on two assumptions.

(1) The rim is thin, almost a lamina.
(2) The number of arms present in the load zone takes change of the load zone angle equally as they appear in the load zone.

The driven pulley of a belt drive rotating clockwise is as shown in Figure 1. The arms of the pulley are designated as OA, OB, OC, OD, OE and OF. Arm OA is assumed to coincide with radial line O1 at any instant of time $t = t_1$. At this instant, four arms OA, OB, OC and OD are in the load zone. Now when OD coincides with O2, at an instant $t = t_2$, only three arms OA, OB and OC will remain in the load zone. Hence, during the time duration $(t_2 - t_1)$, four arms are in the load zone. During further rotation of the pulley, arm OF coincides with O1, at an instant $t = t_3$. Hence, during the time $(t_3 - t_2)$, three arms are in the load zone.

Hence the arm, during its traversal in the load zone, is subjected to varying load.

2.2. TORQUE TRANSMITTED AND ARMLOAD

The belt tension in the active load zone, at an angle ϕ from line of symmetry O1, is given by

$$T = T_s(\mathrm{e}^{\mu\phi i}). \tag{3}$$

Hence, the torque contributed by the portion of the load zone is given by

$$T_q(\mathrm{o} - \phi_i) = T_s(e^{(\mu\phi i)} - 1)r. \tag{4}$$

So, the torque transmitted by the rim to the shaft, through the arms of the pulley is given by:

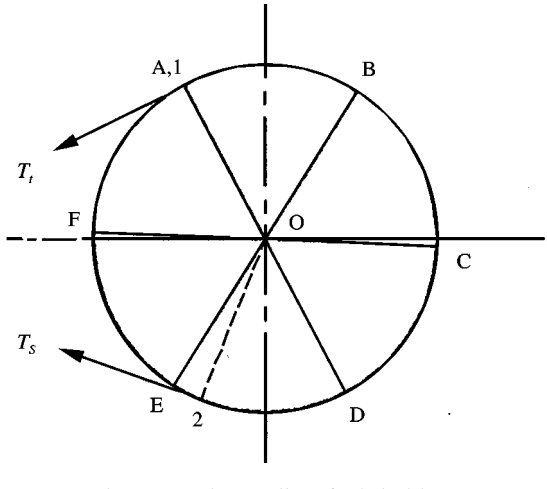

Figure 1. Driven pulley of a belt drive.

(a) *four arms in load zone*

$$T_{q(0-\phi 1)} = (T_1 - T_a)r, \qquad T_{q(\phi 1-\phi 2)} = (T_2 - T_1)r, \tag{5, 6}$$

$$T_{q(\phi 2-\phi 3)} = (T_3 - T_2)r, \qquad T_{q(\phi 3-\phi 4)} = (T_4 - T_3)r. \tag{7, 8}$$

(b) *Three arms in load zone*

$$T_{q(0-\phi 5)} = (T_5 - T_s)r, \qquad T_{q(\phi 5-\phi 6)} = (T_6 - T_5)r, \tag{9, 10}$$

$$T_{q(\phi 6-\phi 7)} = (T_7 - T_6)r. \tag{11}$$

Here $T_4 = T_t$ and $T_7 = T_t$, as $\phi_4 = \phi_7 = \phi$.

The armloads in load zone are as follows:

(a) *Four arms in load zone*

$$F_1 = F_b(e^{\mu\phi 1} - 1), \qquad F_2 = F_s(e^{\mu\phi 2} - 1), \tag{12, 13}$$

$$F_3 = F_s(e^{\mu\phi 3} - 1), \qquad F_4 = F_s(e^{\mu\phi 4} - 1), \tag{14, 15}$$

(b) *Three arms in load zone*

$$F_5 = F_s(e^{\mu\phi 5} - 1), \qquad F_6 = F_s(e^{\mu\phi 6} - 1), \tag{16, 17}$$

$$F_7 = F_s(e^{\mu\phi 7} - 1). \tag{18}$$

Equations (12)–(18) give the expressions for armloads while travelling in the load zone. The graph for this arm load variation as a function of time is as shown in Figure 2 (by converting angle scale to time scale by the expression $t = \phi/\omega$).

3. EQUIVALENT SPRING–MASS–DAMPER SYSTEM

The arm of a pulley is thus subjected to varying load as shown in Figure 2. This loading pattern is achieved subject to some assumptions as discussed in section 2.1. We want to find vibration response of the arm of the pulley subjected to this varying load. We also want to get a cursory idea of the maximum stress due to vibration. As a first attempt, we would like to make a few more assumptions.

1. The arm is considered as a cantilever beam fixed at the hub as shown in Figure 3.
2. The mass of the arm is assumed to be concentrated at the tip, i.e., at the rim of the pulley.
3. The damping present in the arm, called structural damping, is considered in terms of equivalent viscous damping.
4. The stiffness of cantilever at the tip is considered as equivalent spring stiffness.

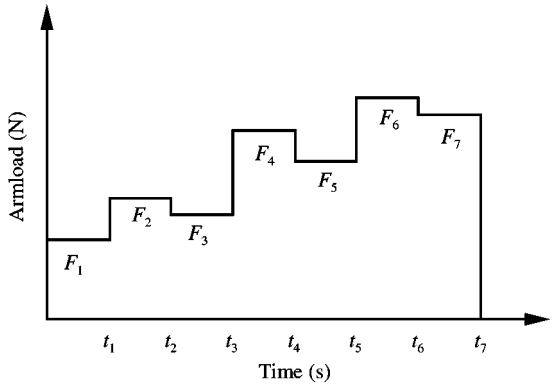

Figure 2. Variation of armload as a function of time.

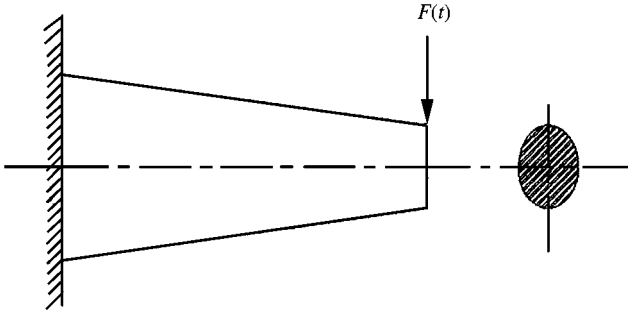

Figure 3. Arm of a belt drive pulley.

3.1. EQUIVALENT MASS

The equivalent mass of the arm is given by [8]

$$M_{eq} = (mr_g)/l. \tag{19}$$

Here the mass of the rotating arm is transferred to its tip by equation (19).

3.2. EQUIVALENT SPRING STIFFNESS

For a cantilever beam subjected to a load at the tip [9], the stiffness is given by

$$K_{eq} = 3EI/l^3. \tag{20}$$

3.3. EQUATION OF ARMLOAD

The arm of the pulley is subjected to loading pattern $F(t)$ as shown in Figure 2. Here the pattern can be analyzed as a combination of step input followed by shifted step input [9]. This unit step function is defined as

$$u(t - t_i) = \begin{cases} 1, & t > t_i, \\ 0, & t < t_i, \end{cases} \quad t_i \geqslant 0. \tag{21}$$

The equation for $F(t)$ is given by

$$F(t) = F_1u(t) + (F_2 - F_1)u(t - t_1) - 2(F_2 - F_3)u(t - t_2) + (F_4 - F_3)u(t - t_3)$$
$$- 2(F_4 - F_5)u(t - t_4) + (F_6 - F_5)u(t - t_5) - 2(F_6 - F_7)u(t - t_6) - F_7u(t - t_7). \quad (22)$$

3.4. EQUIVALENT VISCOUS DAMPING

In this case, the structural damping inside the material of the beam can be modelled as equivalent viscous damping [9, 10]. Structural damping information is well compiled by Lazen [11]. But all the values of loss coefficients, with which we can find equivalent viscous damping, are valid for harmonic excitation. Our excitation, as given by equation (22), being different from harmonic excitation, it is difficult to calculate the exact value of structural damping. Hence, only equivalent viscous damping is assumed varying from 0·0 to 5·0. Higher values of equivalent viscous damping ($> 1{\cdot}0$) are considered for beams, because of the presence of high damping.

The equivalent viscous damping coefficient is hence given by

$$C_{eq} = M_{eq}2\xi\omega_n,$$

i.e.,

$$C_{eq}/M_{eq} = 2\xi\omega_n, \quad (23)$$

where

$$\omega_n = \sqrt{(K_{eq}/M_{eq})}. \quad (24)$$

3.5. EQUATION OF MOTION OF EQUIVALENT SYSTEM

The equivalent spring, mass and damper system as shown in Figure 4, has the following governing differential equation of motion:

$$M_{eq}\,\mathrm{d}^2x/\mathrm{d}t^2 + C_{eq}\,\mathrm{d}x/\mathrm{d}t + K_{eq}x = F(t). \quad (25)$$

Substituting equations (19), (20), (22)–(24) into equation (25) and solving the differential equation (25) by by Laplace transform method, with all initial conditions set to zero, we get

$$x(t) = (Ae^{\alpha t} + B\mathrm{e}^{\beta t})/M_{eq}[F_1u(t) + (F_2 - F_1)u(t - t_1) - 2(F_2 - F_3)u(t - t_2)$$
$$+ (F_4 - F_3)u(t - t_3) - 2(F_4 - F_5)u(t - t_4) + (F_6 - F_5)u(t - t_5)$$
$$- 2(F_6 - F_7)u(t - t_6) - F_7u(t - t_7)], \quad (26)$$

where A and B are coefficients of partial fractions of equation,

$$1/(s^2 + C_{eq}s/M_{eq} + K_{eq}/M_{eq}) = 1/[(s - \alpha)(s - \beta)] = A/(s - \alpha) + B/(s - \beta) \quad (27)$$

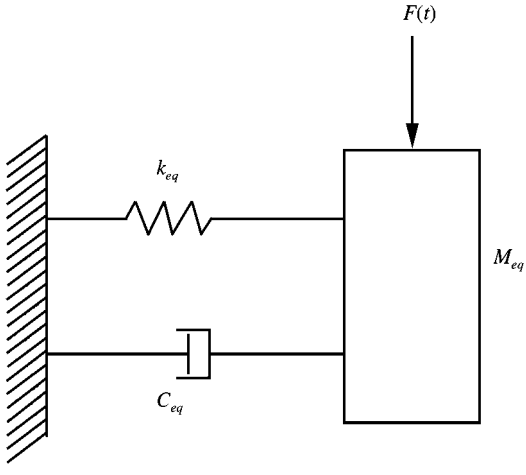

Figure 4. Equivalent spring, mass and damper system.

with

$$\alpha = ((-C_{eq}/M_{eq}) + \sqrt{((-C_{eq}/M_{eq})^2 - 4K_{eq}/M_{eq}))/2},$$

$$\beta = ((-C_{eq}/M_{eq}) - \sqrt{((-C_{eq}/M_{eq})^2 - 4K_{eq}/M_{eq}))/2}. \quad (28)$$

A and B are calculated by writing a program for partial fractions.

Substituting equation (28) into equation (26), we get the response of the system.

3.6. STRESS UNDER VIBRATION

The arm is subjected to varying load, hence it is subjected to stress under vibration. In order to calculate the stress under vibration, we have to first find out the maximum static stress given by

$$S_{st} = (Fl)/Z. \quad (29)$$

The equivalent dynamic force required for calculating the dynamic stress is given by

$$F_v = 3EIy/l^3, \qquad S_{dy} = (F_v l)/Z. \quad (30, 31)$$

So the stress under vibration is given by

$$S_{vb} = S_{dy} - S_{st}. \quad (32)$$

3.7. NATURAL FREQUENCY

The arm of the pulley is assumed here as a tapered cantilever beam. In the present discussion, we have further assumed it to be an equivalent spring, mass and damper system. In order to check the accuracy of the equivalent spring, mass and damper system, we have to find the natural frequency of the tapered cantilever beam, for comparison [12–17].

3.7.1. *Equivalent spring, mass and damper system*

The natural frequency of the equivalent spring, mass and damper system is given by equation (24). If we substitute equations (19) and (20) into equation (24), we get

$$\omega_n = \sqrt{(3EI)/(M_{eq}l^3)}. \tag{33}$$

3.7.2. *Dunkerley's method*

By Dunkerley's method for a massless cantilever, with equivalent mass at the tip of the cantilever, the natural frequency is given by [17]

$$\omega_{n=}\sqrt{2{\cdot}4336EI/M_{eq}l^3}. \tag{34}$$

3.7.3. *Gains and Voltera theory*

Gain's and Voltera [15] have developed tables to calculate natural frequencies of cones, truncated cones and wedges. Taking the line of centers of the cross-sections of the bar in the equilibrium position as the X-axis of Cartesian co-ordinate system XYZ, the Y-axis being in the direction of vibration (see Figure 5), if $A(x)$ denotes the area of cross-section, $r(x)$ the radius of gyration of a generic section about an axis through its center parallel to the Z-axis, y the transverse displacement of the center of the section, the equation of motion according to the Bernoulli–Euler theory is

$$\rho A(x)(\partial^2 y(x,t)/\partial t^2) = -\partial^2/\partial x^2[EA(x)r^2(x))(\partial^2 y(x,t)/\partial x^2)]. \tag{35}$$

In this paper, the lower and upper bounds of natural frequencies along with average values are given [15]. A suitable value of the natural frequency as per our condition, i.e., for a tapered cantilever beam with elliptical cross-section is given by

$$\omega_{n=}\sqrt{4{\cdot}6240EI_h/\rho A_h l^4}. \tag{36}$$

3.7.4. *Gains and Voltera theory* (*with transverse shear and rotary inertia*)

Lee [14] has considered the effect of transverse shear and rotary inertia, for the first time, to find the natural frequencies of a tapered cantilever beam. This theory was used by Gains

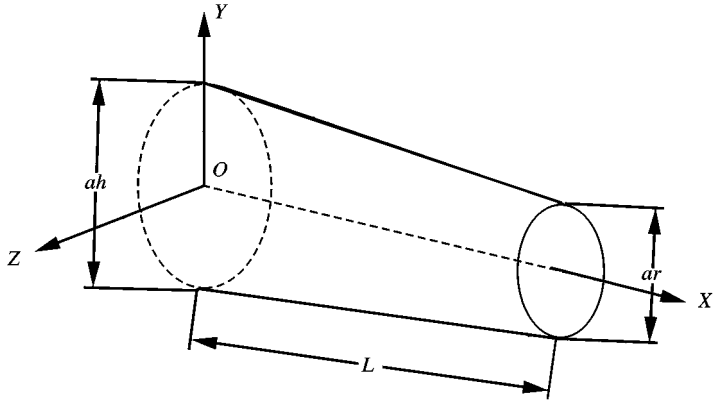

Figure 5. Tapered cantilever beam in XYZ Cartesian co-ordinate system.

and Voltera [15] and with equation (35), created tables of natural frequencies for a tapered cantilever beam. The equation for natural frequency of a tapered cantilever beam with elliptical cross-section is given by

$$\omega_{n=}\sqrt{4{\cdot}53826EI_h/\rho A_h l^4}. \tag{37}$$

3.7.5. *Rayleigh–Ritz method*

It provides a means of obtaining a more accurate value for the fundamental frequency and it also gives approximations to the higher frequencies and mode shapes. In this method, a series of shape functions multiplied by constant coefficients is used [17]. The coefficients are adjusted by minimizing the frequency with respect to each of the coefficients, which results in n algebraic equations in ω^2. The solution of these equations then gives the natural frequencies and mode shapes of the system. The success of this system depends on the choice of shape functions that satisfy the geometric boundary conditions of the problem.

Here the natural frequency is given by

$$\omega_n^2 = (\{\mathbf{x}\}^{\mathrm{T}}[\mathbf{K}]\{\mathbf{x}\})/(\{\mathbf{x}\}^{\mathrm{T}}[\mathbf{M}]\{\mathbf{x}\}. \tag{38}$$

The natural frequency found by different methods by computer simulation is given in Table 2.

4. COMPUTER SIMULATION

Computer simulation for the system, shown in Figure 4, subject to excitation as shown in Figure 2, was performed for the following set of data. The design of belt drive was performed using the software CADOM [18–21].

The input data are

Input power = 21 kW
Speed of driving pulley = 750 r.p.m.
Speed of driven pulley = 250 r.p.m.

The software gave the following design specification of the flat-belt drive and pulley.

Specification of the driven pulley
Material – ISC 30
Diameter = 1247 mm
Diameter of shaft = 63 mm
Diameter of hub = 172 mm
Length of hub = 94·5 mm
Number of arms = 6.

Cross-section of the arm is elliptical with a taper of 1 in 40.

Arm specifications are
Length of the major axis at the hub = 90 mm
Length of the minor axis at the hub = 45 mm
Width of the rim = 142 mm
Thickness of the rim = 16·24 mm
Crown of the rim = 1.42 mm
Angle of lap = 3·33 rad = 190°

TABLE 1

Uniform armload in specified time interval

Sr.	Time interval (s)	Uniform armload (N)
1	$0–0{\cdot}317^{(-)}$	596·492
2	$0{\cdot}0317^{(+)}–0{\cdot}04222^{(-)}$	836·952
3	$0{\cdot}0422^{(+)}–0{\cdot}0633^{(-)}$	1393·698
4	$0{\cdot}633^{(+)}–0{\cdot}0844^{(-)}$	2069·264
5	$0{\cdot}0844^{(+)}–0{\cdot}0950^{(-)}$	2459·331
6	$0{\cdot}0950^{(+)}–0{\cdot}1267^{(-)}$	3883·699
7	$0{\cdot}1267^{(+)}$	3883.699

TABLE 2

Natural frequency of equivalent spring, mass and damper system and tapered cantilever beam by different theories

Theory	ω_n^2	ω_n (rad/s)
Equivalent spring, mass and damper system	$3EI/M_{eq}l^3$	670
Dunkerley's method	$2{\cdot}4336EI/M_{eq}\,l^3$	600
Gain and Voltera theory (with elementary beam equation) [15, 16]	$4{\cdot}6240EI_h/\rho A_h l^4$	242·5
Gain and Voltera Theory (with transverse shear and rotary inertia) [15, 16]	$4{\cdot}53826EI_h/\rho A_h l^4$	240·2
Rayleigh–Ritz method [17]	$(\{\mathbf{x}\}^{\mathrm{T}}[\mathbf{K}]\,\{\mathbf{x}\})/(\{\mathbf{x}\}^{\mathrm{T}}[\mathbf{M}]\,\{\mathbf{x}\})$	257·5

Length of the arm = 529.28 mm
Volume of the arm = $0{\cdot}0011073037229\ \mathrm{m}^3$
Mass density of the material = $7{\cdot}2\times10^3\ \mathrm{kg/m}^3$
Distance of the centroid from the axis of rotation = 0·3178 m
Modulus of elasticity = $9{\cdot}1\times10^4$ MPa
Tension on slack side = 1771·77 N
Tension on tight side = 4978·6678 N

Average moment of inertia of the cross-section of arm = $1{\cdot}005\times10^{-6}\ \mathrm{m}^4$.
Equivalent mass and equivalent stiffness are calculated using equations (19) and (20) as

Equivalent mass = 4·117 kg
Equivalent stiffness = 1·8494 N/m.

Uniform arm loads viz., $F_1, F_2, \ldots, F_7$ for the time zones $(0-t_1)$, $(t_1-t_2)\ldots(t_6-t_7)$ calculated from equations (12)–(18) are as in Table 1.

5. RESULTS

The computer simulation of dynamic and vibration response of arm of driven pulley of the belt drive was performed by using turbo C/C++ ver 3·0 compiler [22]. Equation (26)

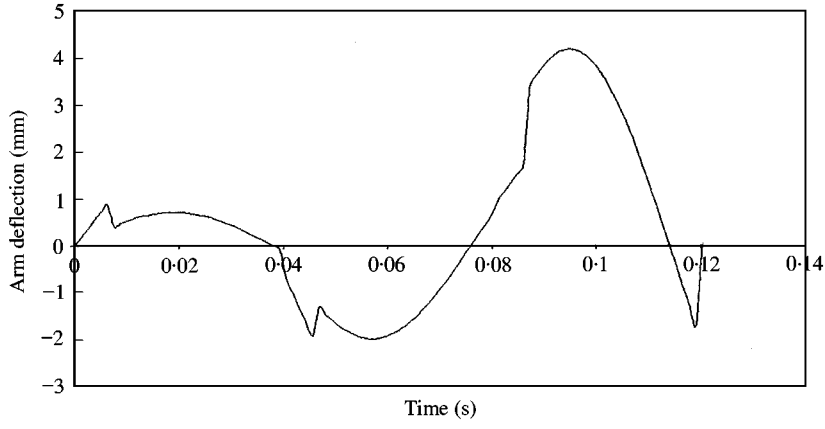

Figure 6. Arm deflection as a function of time for free vibration of the arm: Arm deflection (damping coefficient = 0·1–0·5): ——, Arm deflection (free vibration).

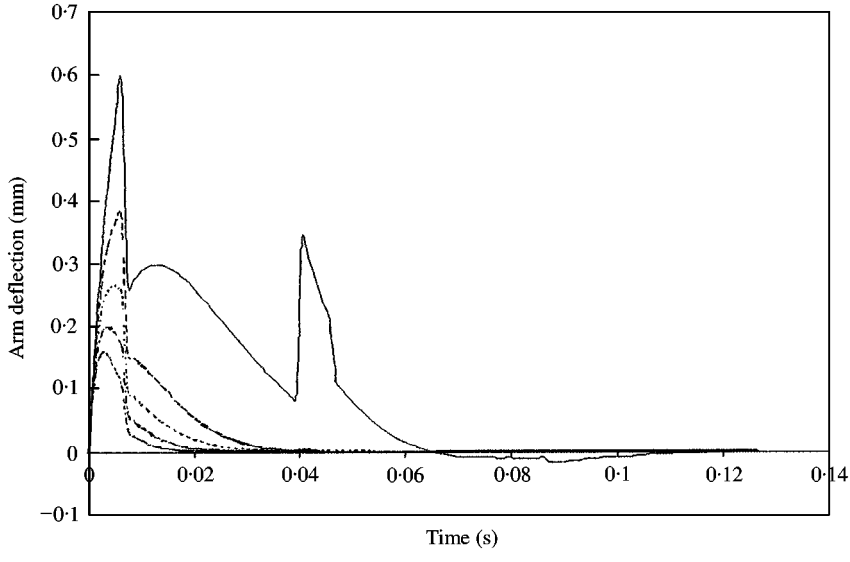

Figure 7. Arm deflection as a function of time for damping coefficient = 0·1–0·5: ——, $x(t)$ for damping = 0·5; – – –, $x(t)$ for damping = 0·1; ·····, $x(t)$ for damping = 0·2; · – · –, $x(t)$ for damping = 0·3; · · – · · ; $x(t)$ for dampuing = 0·4.

was simulated by varying time from 0 to 0·1267 s (i.e., time taken for the traversal of arm in active load zone of 190°) and viscous damping factor ξ from 0 to 1 at one stage and 1–5 at the second stage. The arm deflections $x(t)$ versus time graphs are plotted on the software MS EXEL [23]. Figure 6 shows the variation of $x(t)$ as a function of time for damping coefficient, $\xi = 0$ (free vibration). Figure 7 shows variation of $x(t)$ as a function of time for different values of damping coefficient, ξ varying from 0 to 0·50 in steps of 0·1. Figure 8 shows variation of $x(t)$ as a function of time for different values of damping coefficient, ξ varying from 0·6 to 1·0 in steps of 0·1. Figure 9 shows variation of $x(t)$ as a function of time for different values of damping coefficient, ξ varying from 1 to 5 in steps of 1·0. As in Figures 6–8, the charts of overshoot, settling time, peak time and stress under vibration as a function of damping coefficient, ξ for $\xi = 0$–1·0 are plotted, as shown in Figures 10–13.

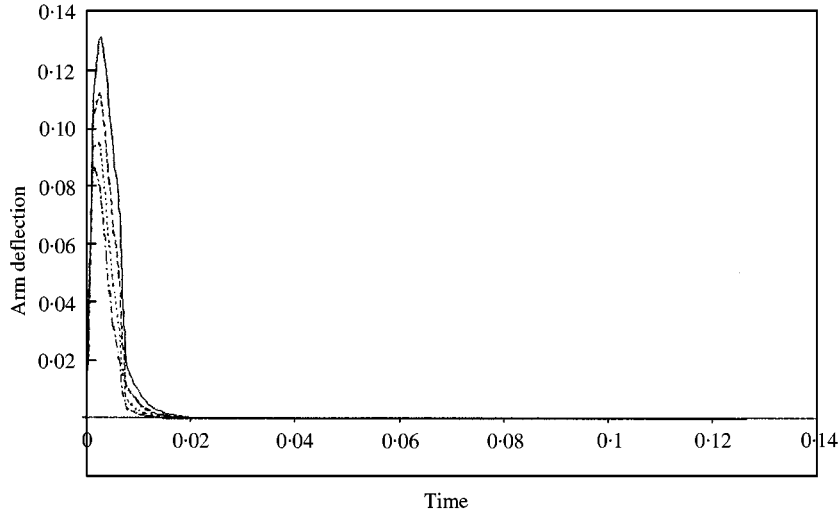

Figure 8. Arm deflection as a function of time for damping coefficient = 0·6–1·0: ——, $x(t)$ for; – – –, $x(t)$ for; ·····, $x(t)$ for; – · – · –, $x(t)$ for; – · · –, $x(t)$.

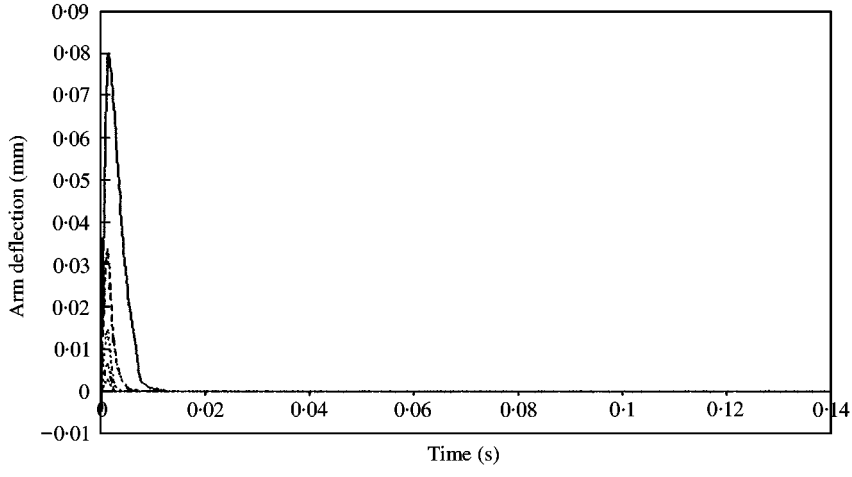

Figure 9. Arm deflection as a function of time for damping coefficient = 1·0–5·0: ——, $x(t)$ for damping = 1; – – –, $x(t)$ for dampuing = 2; ·····, $x(t)$ for dampuing = 3; – · – · –, $x(t)$ for dampuing = 4; – · · –; $x(t)$ for dampuing = 5.

6. DISCUSSION OF RESULTS

6.1. OBSERVATIONS REGARDING THE VIBRATION RESPONSE OF THE EQUIVALENT SPRING, MASS AND DAMPER SYSTEM

The following observations can be made from Figures 6–13.

(1) From Figure 6, for $\xi = 0$, the response is highly oscillatory and the settling time is large. Stress under vibration is tensile.
(2) From Figures 7 and 8, for $\xi = 0{\cdot}1$–$1{\cdot}0$, the response is highly oscillatory in the lower range and sluggish in the higher range ($\xi > 0{\cdot}8$). The overshoot, settling time and peak

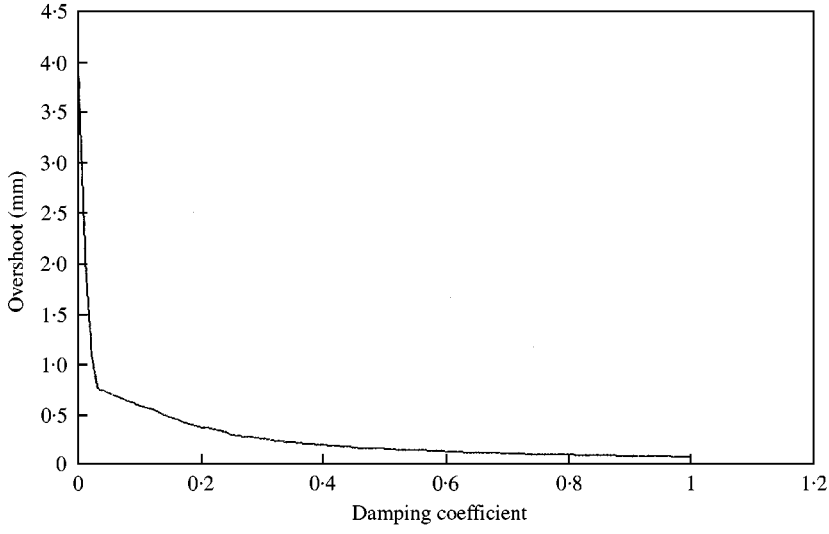

Figure 10. Overshoot as a function of damping coefficient = 0–1·0.

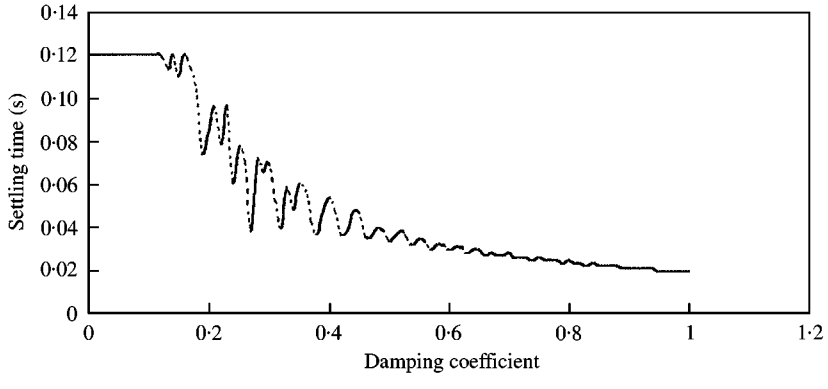

Figure 11. Settling time as a function of damping coefficient = 0–1·0.

time values go on decreasing as damping increases. For very small damping, i.e., $\xi < 0{\cdot}14$, higher harmonics get excited. After $\xi > 0{\cdot}14$, only the principal harmonic is excited. The stress under vibration is compressive and increasing with ξ.

(3) For $\xi = 1{\cdot}0$, the response is sluggish and the overshoot and settling time is very small.

(4) From the plot of settling time versus ξ, it is observed that for a small change in ξ, there is a large change in settling time. Hence, there are dotted segments in these characteristics [24].

(5) For $\xi > 0{\cdot}14$, the system settles very quickly with only the principal harmonic getting excited. This type of step loading hence behaves like the Posicast control system [24]. This type of loading with step input followed by delayed step input allows the system to settle quickly. Conversely, the arm belt drive pulley, with a very high damping factor, is not subjected to large oscillations in practice. So the failure of the arms is not reported from the industry. So our oversimplifying assumption of reducing the arm to an equivalent spring, mass, damper system gives us a cursory idea of the dynamic response of arm of the belt drive pulley.

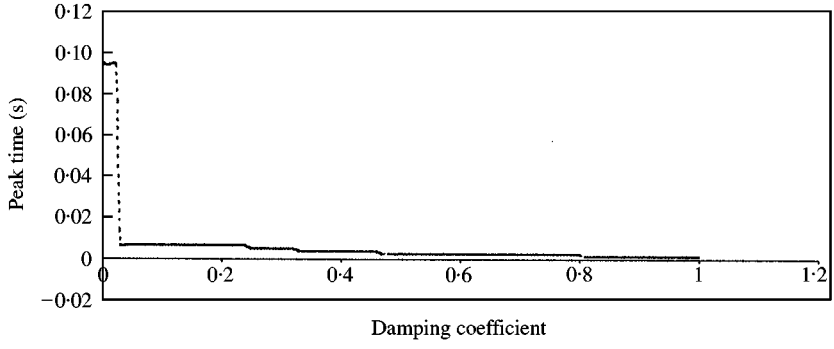

Figure 12. Peak time as a function of damping coefficient = 0–1.

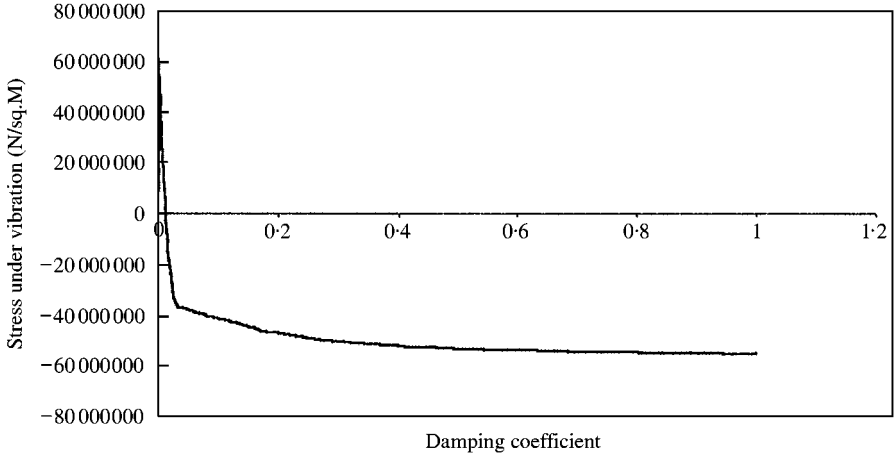

Figure 13. Stress under vibration as a function of damping coefficient = 0–1·0

(6) From Figure 9, for $\xi > 1{\cdot}0$–$5{\cdot}0$, the nature of response is almost the same, with the system becoming more sluggish as damping increases. This range of ξ is considered keeping in view the high values of structural damping being observed in beams.

6.2. OBSERVATIONS REGARDING ACCURACY OF EQUIVALENT SPRING, MASS AND DAMPER SYSTEM FROM THE TABLE OF NATURAL FREQUENCIES

(1) From Table 2 it is observed that the natural frequency of equivalent spring, mass and damper system is very high as compared to the last three methods. The reason for this higher value is associated with our oversimplifying assumptions of,

1. The rim as a lamina,
2. The distributed mass of the system being assumed to be concentrated at the tip of the beam.
3. The stiffness of the beam considered on the basis of deflection at the tip.

(2) In Dunkerley's method, the cantilever is assumed as massless and the mass is assumed to be concentrated at its tip. Hence, the natural frequency comes out to be higher.

(3) In the Gains and Voltera theory, natural frequency, using elementary beam theory, is smaller than the equivalent spring, mass and damper system. This is because it considers the mass and stiffness of the whole system to be distributed.
(4) In the Gains and Voltera theory, rotary inertia and transverse shear are considered to calculate the natural frequency. Hence, this approach gives a lesser and more correct value of natural frequency.
(5) In the Rayleigh–Ritz method, natural frequency is calculated by assuming a suitable shape function. Using CSA/NASTRAN and FEMAP, finite element software, natural frequency of the system is calculated [25, 26] In this software, the arm model is created, discreitized using a tetrahedron element, material parameters and boundary conditions are supplied. Using the Rayleigh–Ritz method, the program calculates the natural frequency. This value is slightly higher than that calculated using (3) and (4), because the tetrahedron element is stiffer.

So far, the vibration response of the arms of pulleys in a belt drive has not yet been reported in the literature. This paper is the first attempt. Hence, this investigation aims at getting a cursory idea of the maximum stress under vibration. Obviously, under the present oversimplifying assumption, only that cursory idea is obtained. From Table 2, it is hence observed that the equivalent spring, mass and damper system considered in this paper is a crude approximation. This problem will be analyzed using the second and third approach mentioned in the problem formulation. Experimental verification of these results will be done in future work.

REFERENCES

1. J. E. SHIGLEY and L. D. MITCHELL 1983 *Mechanical Engineering Design*. Japan: McGraw-Hill Book Company.
2. T. C. FINBANK 1972 *American Society of Mechanical Engineers, paper no.* 72-*PTG*-21. *Mechanics of flat belt drive.*
3. L. M. VALADIMIN and J. B. HARTMAN 1983 *Machine Design*. Delhi: CBS Publisher.
4. E. W. STANTON 1965 *Machine Design*. Mumbai, India: D. B. Taraporwala Sons and Co. Pvt. Ltd.
5. L. S. MARK 1950 *Mechanical Engineers Handbook*. New York: McGraw-Hill Book Co. Inc.
6. M. SARAPH, A. MIDHA and J. C. WAMBOLD 1983 *Transactions of American Society of Mechanical Engineers, Journal of Mechanism, Transmission and Automation in Design* **105**, 400–406. *Stress analysis of mechanical sheaves and pulleys.*
7. J. P. MODAK, *et al.* 1991 *Eighth World Congress on the Theory of Machines and Mechanisms, Prague, Czechoslovakia*, 87–90. *Load variation of the arm of the belt drive pulleys.*
8. E. KREYSZIG 1983 *Advanced Engineering Mathematics*. New Delhi: Wiley Eastern Limited.
9. L. MEIROVITCH 1975 *Elements of Vibration Analysis*. New York: McGraw-Hill Book Co.
10. L. MEIROVITCH 1967 *Analytical Method in Vibration*. New York: Macmillan Company.
11. B. J. LAZAN 1968 *Damping of Materials and Members in Structural Mechanics*. Oxford: Pergamon Press.
12. R. P. GOEL 1976 *Journal of Sound and Vibration* **47**, 1–7. Transverse vibration of tapered beams.
13. R. P. GOEL 1976 *Transactions of American Society of Mechanical Engineers, Journal of Applied Mechanics* **44**, 821–822. Vibration of beam carrying concentrated mass.
14. H. C. LEE 1963 *Transactions of American Society of Mechanical Engineers, Journal of Applied Mechanics* **30**, 176–179. A generalized minimum principal and its application to the vibration of a wedge with rotary inertia and shear.
15. J. H. GAINS and E. VOLTERA 1966 *The Journal of the Acoustical Society of America* **39**, 674–679. Transverse vibration of cantilever bars of variable cross sections.
16. J. S. RAO 1986 *Advanced Theory of Vibration*. New Dehi, India. Wiley Eastern Publication.
17. W. T. THOMSON 1988 *Theory of Vibration with Applications*. Delhi: CBS Publishers.
18. P. M. SINGRU *et al.* 1997 *Proceedings of National Seminar on Emerging Trends in Design Engineering, Organized by Institution of Engineers* (I), *M. N. R. Engineering College, Allahabad India*, I26–I36. Computer aided design of mechanical systems.

19. P. M. SINGRU *et al.* 1998 *Proceedings of National Conference on Intelligent Manufacturing Systems—A Technology Watch, Coimbatore Institute of Technology, Coimbatore, India*, D1.1–D1.8. Computer aided design of mechanical systems (CADOMS) ver. 3.0.
20. P. M. SINGRU *Manual of CADOM* (unpublished).
21. P. M. SINGRU and A. ALIAS 2000 *Proceedings of International Conference on Intelligent Flexible Autonomous Manufacturing System Towards Rapid Design Exploration and Optimization, Coimbatore Institute of Technology, Coimbatore, India.* Computer aided design of machines.
22. *Turbo C ver.* 3.0 *Reference Manual.*
23. *MS office* 97 *Reference Manual.*
24. K. OGATA 1986 *Modern Control Systems.* New Delhi, India: Prentice-Hall of India Pvt. Ltd.
25. *CSA/NASTRAN ver.* 97 *Reference Manual.*
26. *FEMAP ver.*5 *Reference Manual.*

APPENDIX A: NOMENCLATURE

T	tension in the belt at any instant in the load zone of the belt N
T_t	tension on tight side, N
T_s	tension on loose side, N
μ	coefficient of friction (for belt–pulley surface)
φ	angle of lap or contact, rad
P	power transmitted, W
$\langle$'102	angle of lap in the active load zone, rad
R	radius of the pulley, mm
t, t_1, t_2, t_3	time instances of positions of arms in the load zones, s
ϕ_i	active angle of the lap at any instant of time t, rad
$\phi_1, \phi_2, \phi_3, \phi_4$	angles equal to $(\phi/4)$, $(\phi/2)$, $(3\phi/4)$ and (ϕ), rad
ϕ_5, ϕ_6, ϕ_7	angles equal to $(\phi/3)$, $(2\phi/3)$ and (ϕ), rad
$T_1, T_2, \ldots, T_7$	belt tensions for $\phi_1, \phi_2, \ldots, \phi_7$ respectively, N
T_q	torque transmitted by portion of the load zone $(0 - \phi_i)$ from 01 to any instantaneous arm position at an angle of ϕ_i
F_1, F_2, F_3, F_4	uniform arm load in the load zone from $(0 - \phi_1), (\phi_1 - \phi_2), (\phi_2 - \phi_3), (\phi_3 - \phi_4)$ respectively, N
F_5, F_6, F_7	uniform arm load in the load zone from $(0 - \phi_5), (\phi_5 - \phi_6)$ & $(\phi_6 - \phi_7)$ respectively, N
ω	circular frequency of the rotating pulley, rad/s
ω_n	natural frequency of the arm of the pulley, rad/s
m	mass of the arm of the pulley, kg
r_g	distance of centroid of the mass of the arm from fixed end, m
l	length of the arm, m
M_{eq}	equivalent mass of the arm, kg
K_{eq}	equivalent stiffness of the arm, N/m
I	average moment of inertia of both end cross-sections, m^4
E	modulus of elasticity of the material of the arm of pulley, N/m^2
$F(t)$	arm load at any instant of time t, N
$u(t - t_i)$	shifted step function
C_{eq}	equivalent viscous damping coefficient
$x(t)$	displacement of the equivalent mass, m
A, B	coefficients of partial fraction of equation (25)
α, β	roots of quadratic equation (26)
ξ	viscous damping factor
S_{st}	static stress in the arm, N/m^2
F	maximum arm load, N
Z	section modulus of the arm (of average c.s.), m^3
S_{dy}	dynamic stress, N/m
Fv	equivalent dynamic force, N
S_{vb}	stress under vibration, N/m^2
V_s	velocity of the belt on slack side, m/s
V_t	velocity of the belt on tight side, m/s

I_h	moment of inertia of arm at the hub, m^4
A_h	cross-sectional area of the hub, m^2
$\{\mathbf{x}\}$	displacement vector
$\{\mathbf{x}\}^T$	transpose of displacement vector
$[\mathbf{K}]$	stiffness matrix
$[\mathbf{M}]$	mass matrix
ρ	mass density of the material, kg/m^3
$A(x)$	area of cross-section, m^2
$r(x)$	radius of gyration of a generic section about an axis through its center parallel to the Z-axis, m
y	transverse displacement of the center of the section, m